



# Effects of static magnetic field on dye extracted from *Anchusa-Italica* through optimization the optoelectronic properties

Fatima H. Malek<sup>a</sup>, Tahseen Alaridhee<sup>a,\*</sup>, Abdullah A. Hussein<sup>a</sup>, Arwa H. M. AL-Saeed<sup>b</sup>

<sup>a</sup>Department of Material Science, Polymer Research Centre, University of Basrah, Iraq

<sup>b</sup>Department of chemistry, College of Science, University of Basrah, Iraq

---

## Abstract

The dye extracted from the plant is already well used in optoelectronic applications for its easy and safe handling. This study is to demonstrate the effect of magnetized distilled water on dye extracted from *Anchusa-Italica* flowers. The results of its optoelectronic behavior reveal that the use of magnetized water in the extraction process results in different and better properties than processes in which ordinary water was used. The structural analysis of *Anchusa-Italica* dye thin-film was performed using the Fourier-transform infrared technique (FT-IR). The optical responses, such as the absorption coefficient, absorption spectra, both standard and refractive indices, and electronic properties (optical energy gap) were studied using Ultraviolet-Visible transmittance spectra range 300–900 nm. The calculated energy band gap of the dye extracted using magnetized water was decreased from 3.23 to 2.35 eV and turned into the preferred direct band gap to make a useful contribution to optical sources. The optical absorption spectra of the dye extracted using magnetized water appear to have a better efficiency compared to that extracted with ordinary water. A significant evolution in the absorption coefficient was obtained by employing magnetized water to extract the dye. The magnetized extraction process also modified the electronic transmission values (indirect to direct). The effect of magnetized water on the resonance mode and transparent indication was deduced by studying the complex refractive index. An increase appeared in the spectrum of the absorption index at a wavelength of 570 nm, whereas a small attenuation coefficient was observed as well. The important effects of magnetized dye extraction will highly benefit the field of optoelectronic applications.

**Keywords:** static magnetic field, optical absorption spectra, green materials, optical properties, optical energy gap

---

\*Corresponding author

Email addresses: [fatima.malk@uobasrah.edu.iq](mailto:fatima.malk@uobasrah.edu.iq) (Fatima H. Malek), [tahseen.alaridhee@uobasrah.edu.iq](mailto:tahseen.alaridhee@uobasrah.edu.iq) (Tahseen Alaridhee), [aahaat28977@yahoo.com](mailto:aahaat28977@yahoo.com) (Abdullah A. Hussein), [arwa.mahmood@uobasrah.edu.iq](mailto:arwa.mahmood@uobasrah.edu.iq) (Arwa H. M. AL-Saeed)

Received: February 2021    Revised: April 2021

2010 MSC: Primary 90C33; Secondary 26B25.

---

## 1. Introduction

The different colours of flowers inspired the scientist to employ natural dye extract to explore and develop optoelectronic materials [1, 2, 3]. Natural dyes are being considered increasingly important, as they reduce global environmental pollution, can be easily extracted, are widely available, are made through green production and are environmentally friendly [4, 5]. These characteristics support their application in many fields, such as dye-sensitized solar cells [6], natural textile dyes [5], pH indicators [7, 8] and optoelectronic devices [9]. The researchers of this study focused on improving the performance of the photoconduction limit by making the natural dyes exhibit behavior like semiconductor materials. The considerable importance of natural dyes in photosensitizers, for example, is mainly a result of their light gain and high absorption efficiencies. The interesting photoelectronic properties of the dye originate from the interaction of the electronic structure of the dye with white light and variations in frequencies. Therefore, the transmitted or reflected light leads to maximum absorbance in the spectrum [10, 11]. Consequently, attempts were made to use natural dyes/pigments as semiconductors by increasing the capability of the electron injection between the valence and conduction bands. One of the most important sources of natural dye is flowers because of their composition elements, such as anthocyanins, chlorophyll, cyanidins, tannins and their derivatives (chalcones, betalains, carotenoids, etc.) [12, 13, 14]. Anthocyanin is the main component of most cyanic colours, including the reds, violets, dark blues and scarlets of the flavonoids of flowers, fruits and leaves [15].

The greatest advantage of the dyes is that the extraction can be easily performed using distilled water. Therefore, the electronic structure can be controlled via magnetization, and hence allows for optimization of the photoelectronic properties. Several studies have shown that the changes in optics and physical properties arise as water is exposed to the magnetic field [16, 17, 18, 19, 20, 21, 22, 23, 24]. Thereafter, a very large number of theoretical publications based on the concept of quantum theory have been devoted to studying the effect of the magnetic field on physicochemical properties [25, 26, 27]. The magnetic field modified the physicochemical properties of the prepared laboratory solution across magnetic flux density ranges, from 0.1 to 0.8 T [28, 29, 30]. Water can be magnetized using a permanent magnet without additional energy.

Another intrinsic property is the ability of the magnetic field to weaken the intra-cluster hydrogen bonds, thus breaking the massive clusters into smaller and stronger inter-cluster hydrogen bonds [23]. The van der Waals molecules in water are also broken under the magnetic field effect, as reported in [31]. As a result of the magnetized water, it may contribute to increasing the effectiveness of dye extraction due to the formation of small clusters and the viscosity of water that leads to better absorption by the plant and faster entry through the cell membranes, respectively [16, 23]. To our knowledge, very little research has been conducted in this context, particularly the magnetized water uses in the processing of the dye extraction. Based on the characteristics of natural dye and magnetized water, this study is devoted to exploiting a static magnetic field in the extraction process of the *Anchusa-Italica* (*A. italica*) flower. Then, the excreted dye is investigated to measure several of its aspects, including the optoelectronic properties.

## 2. Materials and methods

### 2.1. Natural dye extraction

The *A. italica* flowers were collected and purchased from a local market and purified in a laboratory in Iraq. The petals of the flowers were first washed under running tap water to rub down

and remove any dust particles before proceeding with the extraction. The purified layers were then kept in a dark and dry place at room temperature for 10 days before being crushed in a mortar. The powdered petals were soaked in distilled water in a closed container to prepare it for use as an aqueous extract ore. About 10 g of the powdered flower was placed in 100 ml of distilled water. Then, the solution was placed in a water bath to make sure that it had been saturated enough. In order to study the magnetic field effect, the extraction process was repeated in the same manner as described above, but the repetitions were performed with the addition of the magnetization process that will be explained in the next paragraph. Subsequently, the extracted dye was filtered using a filter paper with a scale of 60 g/m<sup>2</sup> and 0.20 mm thickness, then left to cool for 48 hours and kept in a suitable container at room temperature.

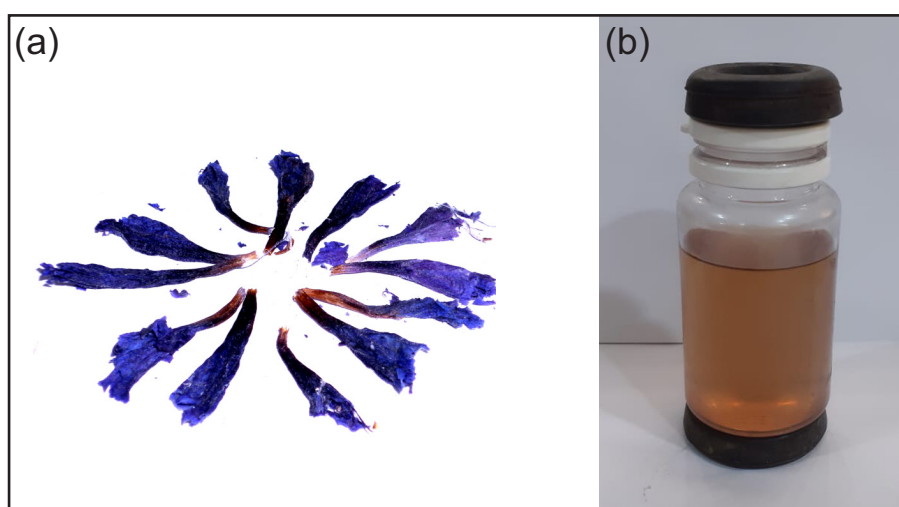


Figure 1: (a) The *Anchusa-Italica* flower and (b) the setup of two torus magnets on the top and bottom the extracted dye.

### 2.2. Aqueous solution magnetization

For the magnetic exposure, a covered plastic container filled with the extracted dye was placed and centred between two permanent magnets with a diameter of 5 cm (KC-70C) purchased at a local market in Iraq. The strength of the magnetic field localized at the central point between the two magnets (see Figure 1) and at room temperature was measured using an SE-9906 A digital Gauss/Tesla meter. The maximum magnetic flux density of the two torus magnets was  $1000 \pm 20\%$  mT with an intensity of 0.20 T. Distilled water was exposed to the static magnetic field for a period not exceeding 60 minutes.

### 2.3. Preparation of thin-film

The final product was cast on a glass slide of dimension  $2 \times 2$  cm, which was cleaned with acetone and distilled water, dried at 60°C, and then placed in an electric oven for 15 minutes. The casting process was performed through the spin coating method for several rotations (1000 rpm/min). The coated glass slides of *A. italica* were uniform with a thickness of 200 nm and pure enough to ensure their suitability.

### 3. Characterization techniques

#### 3.1. Chemical profile

Several qualities of the extracted dye were performed to determine the chemical content. Dragendorff and Mayer reagents were used to detect and ensure the presence of alkaloids. The triterpene and sterile components were tested using the Lieberman-Burchard test, whereas the amines group, tannin, and carbohydrates were detected using the ninhydrin 1%, lead acetate 1% and Molisch's reagent, respectively. Furthermore, the presence of tannin and vitamin E was detected in the *A. italica* aqueous extract according to the lead acetate test. All the tests performed in the aqueous extract are listed in table 1.

#### 3.2. Stretching mode analysis

The Fourier transform infrared spectrum scope technique (FT-IR) was used to provide information about the characteristic band of the functional group. The chemical structure of the *A. italica* dye powder was identified and recorded as KBr disk. The active group recorded in the mid infrared (MIR) range (4000–400)  $\text{cm}^{-1}$  are presented in Figure 2. The interaction between electromagnetic radiation and matter in the molecule is portrayed as different absorption peaks depicted in the spectrum of Figure 2. The broad peak in the spectrum represents the O–H stretching vibration at 3386  $\text{cm}^{-1}$ . The peak observed at the frequency of 2927  $\text{cm}^{-1}$  follows the saturated C–H stretch. The absorption peaks of O–H and C–H was caused due to the presence of flavonoids, fatty acids, saponins, and tannins. Additionally, the weak stretching vibration positioned at 1735  $\text{cm}^{-1}$  can be attributed to the carbonyl bond C=O that arises from the variation of polar dipole-dipole interaction. The strong absorption band located at 1631  $\text{cm}^{-1}$  ensures the presence of the conjugated dyeing C=C stretch vibration. Furthermore, the stretching band of C–O exists in two different frequencies: the high vibration appears at 1061  $\text{cm}^{-1}$  due to the  $\text{sp}^3$  orbital, whereas the insignificant peak positioned at 1416  $\text{cm}^{-1}$  is attributed to the  $\text{CH}_2$  bend. The molar ratio M was determined using the following relation:

Table 1: Chemical analyzes of *A. italica* aqueous extract.

Substance	Deragendraoff reagent	Mayer reagent	Ninhydrin 1%	Lead acetate 1%	Lieberman Burch red 1%	Mulish $\text{FeCl}_3$ reagent
<i>A.Itaica</i>	–	–	–	+	–	–

$$M = \frac{W(g)}{W_m(g/mol)} \times \frac{1000}{\text{volume}(ml)} \quad (3.1)$$

where  $W$  and  $W_m$  represent the weight and the molecular weight, respectively.

#### 3.3. Influences of magnetic fields on the characterization of *A. italica* thin-film

In an optoelectronic system, linear optical properties of direct and indirect band gaps are essential. The fundamental properties were measured using a double beam ultraviolet- visible (UV-Vis) spectrophotometer (CE-1800) for wavelengths of 300–900 nm at room temperature. The electronic structure of an organic compound under the influence of a magnetic field was illustrated, and measurements of linear optical parameters on thin-film samples have been made, such as transmittances, absorptions, reflectance, optical energy gap, optical absorption coefficient and excitation factors.

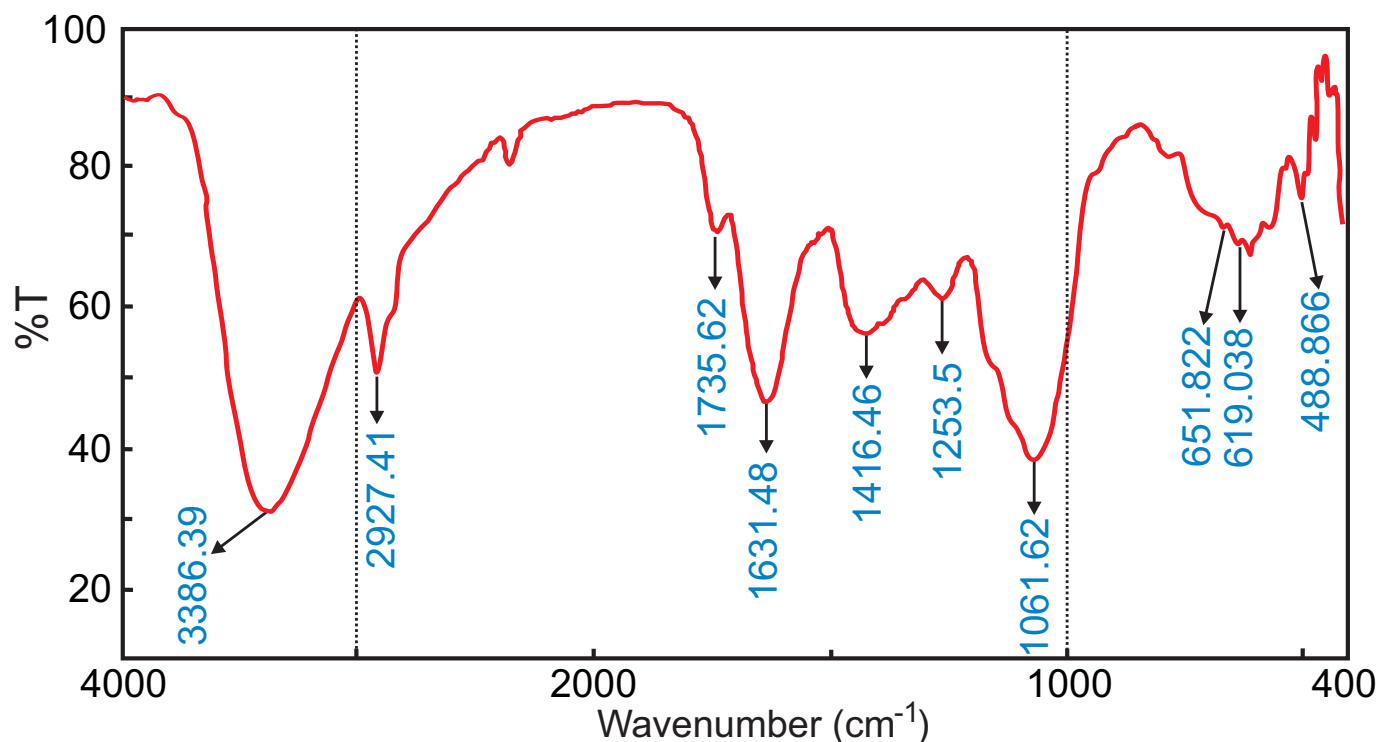


Figure 2: The FT-IR spectra of the extracted *A. italica* dye.

## 4. Results and Discussion

### 4.1. Optical absorbance

The optical absorption spectrum is influenced by many factors, such as the chemical composition, absorbed photon energy, thickness and topography of thin film. In our study, the aqueous extract was affected by the application of the static magnetic field, as we will see later. Absorption spectra were recorded for the magnetized extract of *A. italica* (MEA) and the ordinary extract of *A. italica* (OEA) thin films in the 300–900 nm band. In Figure 3, a comparison between the absorption of the MEA and OEA having the same film thickness is presented. As shown in Figure 3, the maximum absorbance peak of the OEA appears at 310 nm and reaches 30% intensity, whereas the spectral position of the MEA is significantly red-shifted with 20% intensity. Indeed, this decrease in the absorbance value is due to the changes in the polarization of atomic effects occurring in the molecular distributions and the enhanced functionality of the transition dipole moment of electrons. In this context, the photon energy in

visible and UV regions released from organic molecules may include twin or triple bonding  $\pi$ , mono bonding  $\sigma$  and non-bonding n-orbital electrons. These bonds can absorb the energy emerging from the ground state to excited states [32]. The spectra ranging 400–600 nm correspond to the excitation of  $n \rightarrow \pi^*$  [33, 35]. The latter, called R-band, emerges from unsaturated chemical groups (chromophore groups) in a molecule [36].

### 4.2. Optical absorption coefficient

In the band of the absorption region, the absorption coefficient  $\alpha$  becomes very important to determine the type of electronic transfer that occurs in the electronic structure of the material [34]. For this purpose, the absorption coefficient was estimated using the following equation [37]:

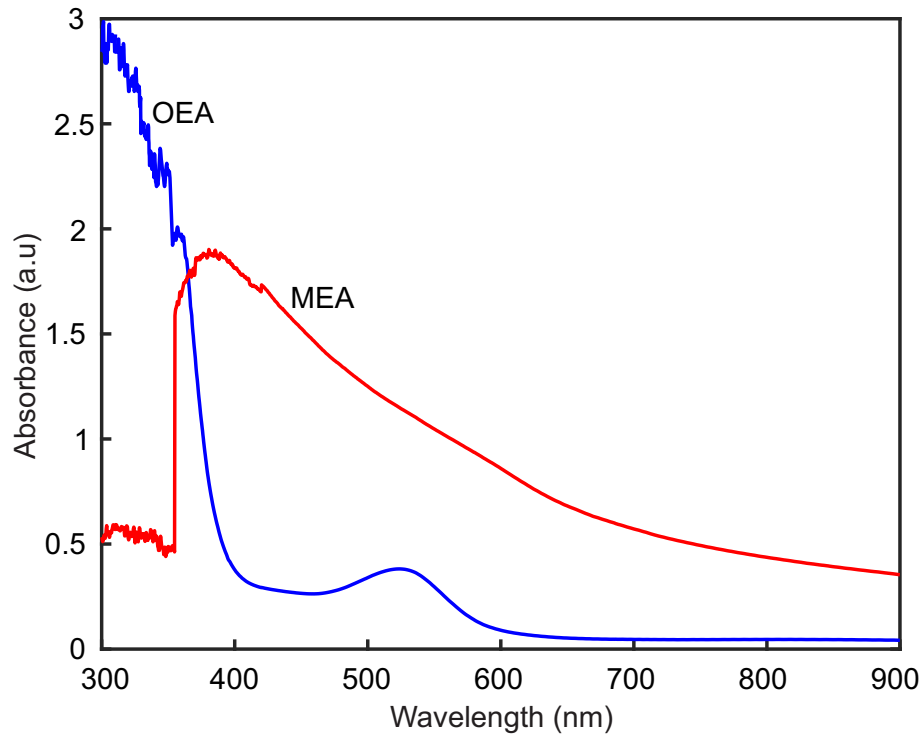


Figure 3: The absorption spectra of magnetized extracted of *A. italica* (MEA) (red curve) and ordinary extracted of *A. italica* (OEA) thin-films (blue curve).

$$\alpha = \frac{1}{d} \ln \left[ \frac{(1 - R)^2}{2T} + \sqrt{\frac{(1 - R)^4}{4T^2} + R^2} \right] \quad (4.1)$$

where  $T$  and  $R$  are the transmittance and reflection, respectively, and  $d$  represents the film thickness. The latter is estimated via the classical method that requires to know the mass of both glass sheet  $m_1$  and the *A. Italica* thin film together with glass substrate  $m_2$  as defined below:

$$d = \frac{m_2 - m_1}{\rho a} \quad (4.2)$$

Where  $\rho$  and  $a$  are the density of *A. Italica* and area of thin film, respectively. Therefore, *A. Italica* thin film has thickness equal to  $d = 195$  nm. The estimated factor  $\alpha$  is frequently used to classifying the optical energy gap, also known as the absorption edge.

The factor  $\alpha$  has been measured for the MEA and OEA having the same film thickness in the 300-900 nm bandwidth (see Figure 4). The results show a significant difference in peak value for which the MEA has greater significance. As can be seen from Figure 4(a), the peak value of the OEA sample is of ( $< 10^4$ ), indicating that the electronic transition between the states was indirect [38]. Correspondingly, for MEA film, the image is completely reversed, leading to direct transmission (see Figure 4(b)). By the same reasoning, these peaks appearing in Figure 4 are a result of the electronic transition  $n \rightarrow \pi^*$  between bonding and anti-bonding molecular orbitals [39, 40]. Consequently, the absorption coefficient acquires its importance by determining the so-called absorption edge or optical energy gap. The latter has a significant role in semiconductors and dielectric materials through controlling the mobility of conduction electrons. The energy gap values can be deduced using intercept  $(\alpha h\nu)^\gamma$  versus  $h\nu$  of the x-axis (i.e.  $(\alpha h\nu)^\gamma = 0$ ) as depicted in Figure 4. The latter result seems evident from the Tauc's relationship, can be calculated using [41]:

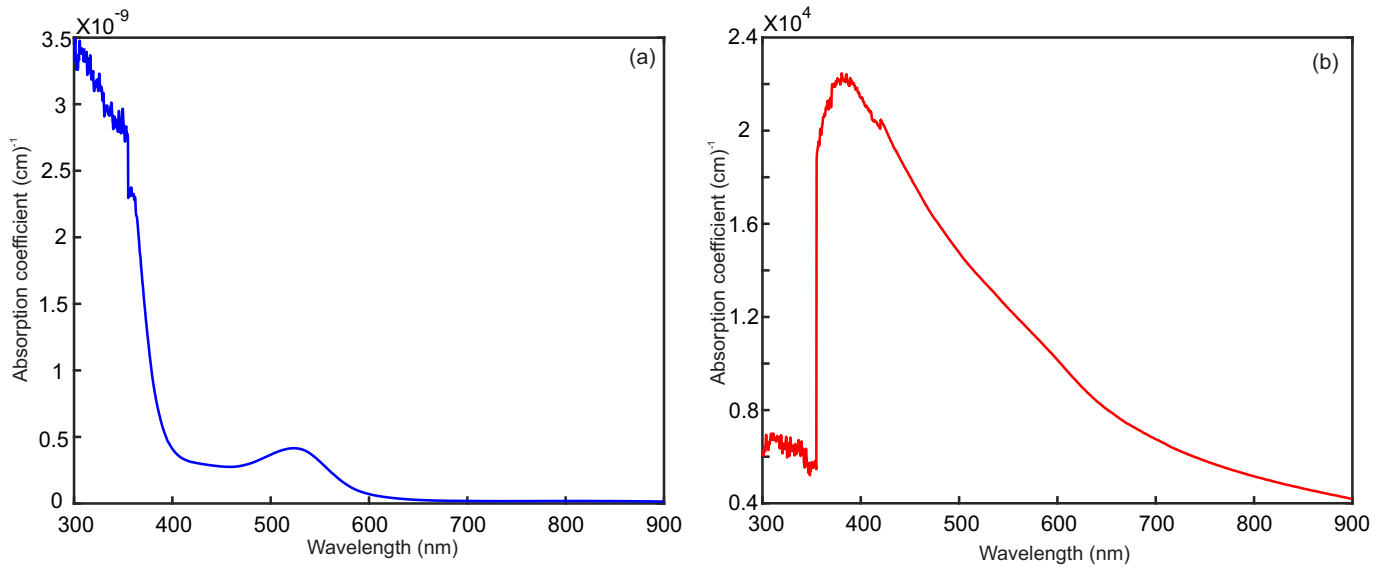


Figure 4: The absorption coefficient  $\alpha$  of the (a) OEA, and (b) MEA samples.

$$\alpha = \frac{A [(hv - E_g)]^\gamma}{hv} \quad (4.3)$$

where  $A$  represents the transition probability dependent constant, and  $\gamma$  is the distribution of the density of states index, which can have different values depending on the transition path (direct transition paths,  $\gamma$  takes values of  $\frac{1}{2}$  and  $\frac{3}{2}$  for allowed and forbidden, respectively, whereas for indirect transition paths, the values are 2 and 3 in allowed and forbidden, respectively).

#### 4.3. Optical energy gap

With regard to the energy gap, an important point is determining the photon contribution in the visible region. These photons are responsible for exciting the electron to atomic energy levels in the conduction band. Therefore, as the energy band gap is small enough, the number of empty states becomes greater in that band. To illustrate the calculation of the band gap energies of thin-films, equation 4.1 mentioned previously is applied to take into account the value of the  $\gamma$  index. As deduced from Figure 4(a), the electronic transition was indirect allowing  $\gamma$  to be replaced with 2.

Figure 5(a) shows that the OEA sample has an energy gap value of  $E_g = 3$  eV. The result obtained in Figure 5(a) is quite possibly due to defects in sample configuration that led to the generation of new localized levels below the natural conduction band. Figure 5(b) shows a significant decrease in the energy gap value of the MEA sample, that is  $E_g = 2.316$  eV. This variation is associated with the OH concentration, as the magnetic field effect in the dye enhances the structure with more molecule's dipoles and coherent energy approaches as well.

#### 4.4. Extinction coefficient and Linear refractive index

Let us now turn to the study of the optical indices  $n$  and  $k$  that are the significant contributory factors in the optical spectra owing to the interband transition of electrons from valance bands to the conduction bands. These two quantities  $n$  and  $k$  represent the phase velocity of the wave material and the diminution of the photon energy by matter electrons, respectively. On the other hand,  $n$  and  $k$  represent the real and imaginary parts of a complex frequency-dependent equation, respectively. In the literature, the study of the  $n$  factor has been associated with different applications, such as

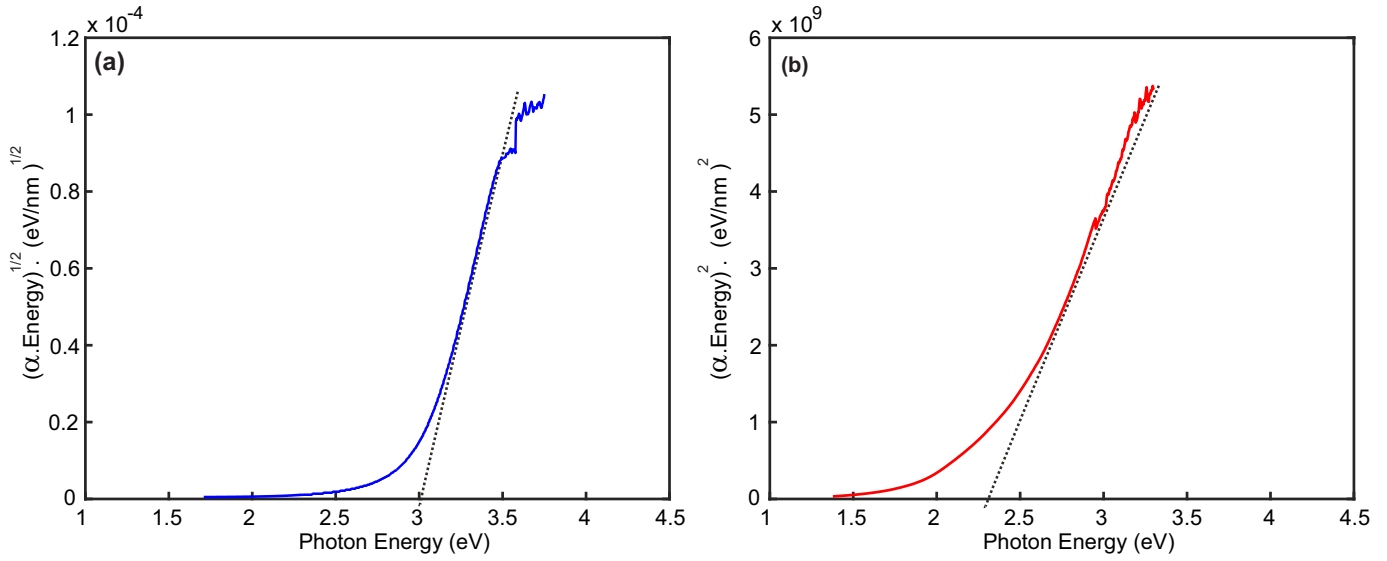


Figure 5: The calculated optical energy gap of (a) OEA, and (b) MEA samples from the  $(\alpha h\nu)^{\frac{1}{2}}$  in a and  $(\alpha h\nu)^2$  in b versus  $h\nu$ .

chemical sensors [42], solar cells [43], optical trapping [44], spectral filters [45], biomedical detection [46]. The two quantities  $n$  and  $k$  can be estimated from the relationships in the following [47]:

$$n = \frac{1 + R}{1 - R} + \sqrt{\frac{4R}{(1 - R)^2} - k^2} \tag{4.4}$$

$$k = \frac{\alpha\lambda}{4\pi} \tag{4.5}$$

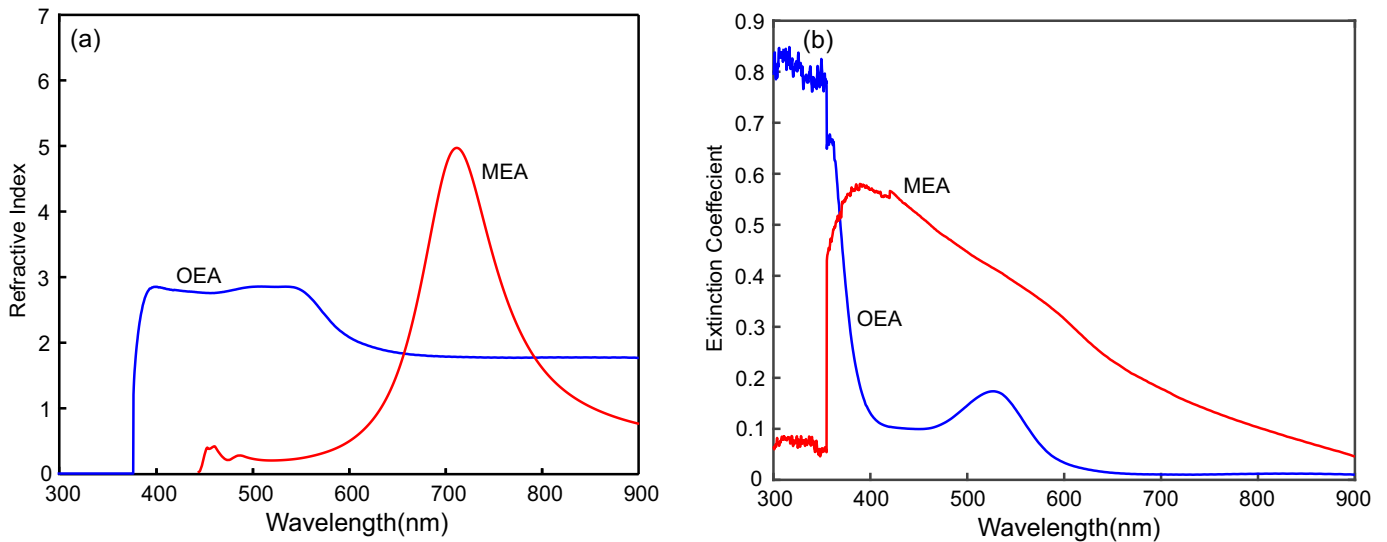


Figure 6: (a) Refractive index and (b) the extinction coefficient of OEA (blue curve) and MEA (red curve) thin-films.

To figure out how to affect the magnetic field on the index  $n$ , Figure 6 shows the relation of index  $n$  versus the wavelength of both the OEA and MEA samples. The findings reveal that there has been a gradual increase in the refractive index of the OEA sample within a range of 370~580 nm (see blue curve in Figure 6(a)). Quasi-stability in the factor  $n$  was noted as the spectrum shifts towards the

red region. In Figure 6(a), an evolution in the refractive index spectrum occurs inside the MEA film at a wavelength of 570 nm (see red curve in Figure 6(a)) continuing the progressive rise in overall bandwidth. The increase in the real part of the refractive index refers to the resonance mode being excited as a consequence of the coupling of collective oscillation with the conduction electrons in a film on which light is incident. On the other hand, the behavior of the real part of the factor  $n$  of the MEA presented in Figure 6(a) (red curve) is demonstrated in the optical response of the absorption spectrum, ensuring the resonance excitation in the MEA sample.

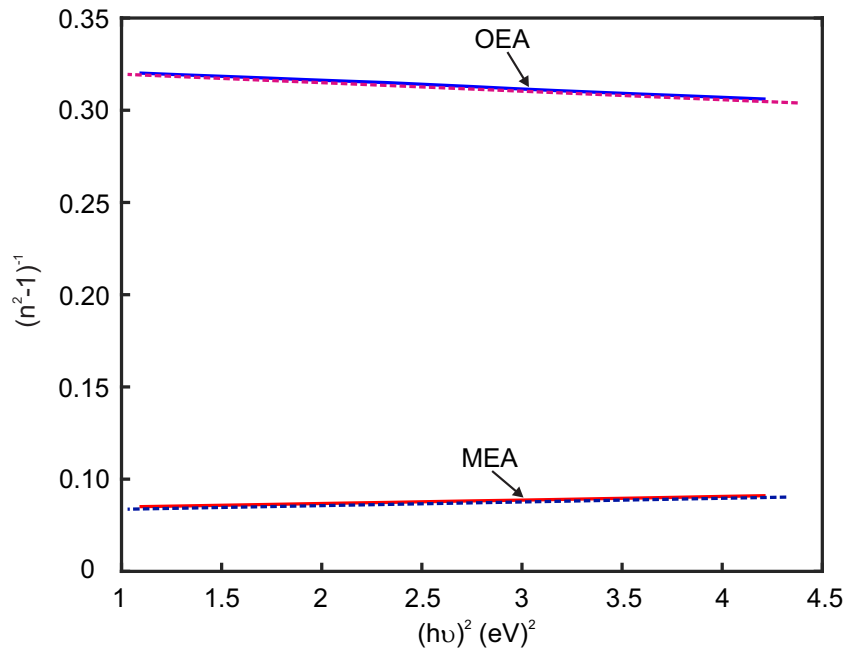


Figure 7: The variation of  $1/(n^2 - 1)$  versus  $(h\nu)^2$  for OEA (blue solid line) and MEA (red solid line) samples.

Depending on equation 4.5, Figure 6(b) investigates the extinction coefficient  $k$  for both samples (OEA and MEA) with the same wavelength range as the  $n$  index. As a result, one can deduce that the absorption index of the MEA sample (see the red curve in Figure 6(b)) clearly exhibits a low spectral response compared with that recorded in the OEA sample. Therefore, this corresponds to low attenuation of light when penetrating the MEA thin-film, which is directly linked to the dispersion properties of the material affected by the polarization effect and dielectric losses.

#### 4.5. Dispersion Photon Energy parameters

Due to the interest in the dispersion refractive index which includes a likely application in designing optoelectronic and optical communication devices, a more detailed study was performed on the samples. The Wemple and DiDomenico (WDD) model [48] illustrates this point clearly by exploiting the single effective properties. The latter is described as frequency-dependent dispersion through the so-called average oscillator energy ( $E_o$ ) and the average oscillator strength of inter-band optical transition ( $E_d$ ). In the WDD model, the refractive index measurements have been treated below the interband absorption edge. The relation between the refractive index and optical energy based on single oscillator can be provided by:

$$n^2 = 1 + \frac{E_o E_d}{E_o^2 - (h\nu)^2} \quad (4.6)$$

Where  $h\nu$  represents photon energy. To verify the experimental configuration of equation 4.6, the plotting of  $1/(n^2 - 1)$  as a function of  $(h\nu)^2$  is required. Linear behavior is obtained by fitting the function through the data (see Figure 7). Thus, the parameters  $E_o$  and  $E_d$  can be estimated directly from the gradient  $(E_o E_d)^{-1}$  and intercept  $(E_o/E_d)$  on the vertical axis. As depicted in Figure 7, a linear fit is produced for both OEA and MEA films to obtain the WDD dispersion parameter values  $E_o$  and  $E_d$ . The latter for the two samples under study are given in table 2. As can be deduced from Figure 7, the  $E_o$  and  $E_d$  of MEA film tend to have values greater than those in OEA film; overall,  $E_d$  value appears to be greater than  $E_o$ . We only mention the parameter values here; more details on this topic can be found in [34, 48, 49, 50, 51], for a full investigation.

Table 2: Dispersion energy parameters of the aqueous extract.

Sample	$E_g(eV)$	$E_d(eV)$	$E_o(eV)$
OEA	3	1.8911	0.422
MEA	2.316	2.9217	0.545

## 5. Conclusion

In summary, the optical response of *A. Italica* dye thin-films in terms of the magnetic field effect was investigated. A comparison was made between the samples to demonstrate the effect of the induced magnetic field on the optical properties. For this purpose, two permanent magnets were used to ensure that the sample under study was well exposed to a magnetic field. Two methods were adopted: chemical profiling and FT-IR techniques. The latter exhibits the spectra measured and the stretching modes in the mid-IR region ( $4000 - 400$ )  $\text{cm}^{-1}$ . The optical parameters, such as the absorbance response, absorption coefficient  $\alpha$ , optical energy gap, refractive  $n$  and extinction  $k$  indices with and without the influence of the magnetic field were studied. The absorption maxima of the magnetized extract of *A. Italica* shifted to the red region compared to that of the normal dye located at a wavelength of 310 nm. This result was obtained due to the variations in the polarization of atoms and the magnetic dipole-momentum of electrons in molecules. In the absorption band, the absorption coefficient for both the OEA and MEA samples was calculated to fix the type of electronic transfer between energy levels. The direct transmission was observed as  $\alpha < 10^4$  in the MEA sample, whereas the OEA sample indicated indirect transmission. The absorption coefficient values were used to estimate the energy gap via Tauc's relationship. Magnetization was able to decrease the optical band gap from 3.23 to 2.316 eV and turn it into a direct band gap. This improvement can be explained by the concept of the chemical bond and coherent energy approaches. The refractive index has dramatically increased in the MEA film starting at a wavelength of 570 nm, whereas the OEA sample exhibited a quasi-stability in that (red) region. The different behavior in refractive index of the two samples is associated with the excitation of the resonance mode. Regarding the extinction coefficient, a very low light attenuation was observed in the MEA sample due to the modification in dispersion properties induced by the magnetic field. Furthermore, the refractive index in terms of dispersion photon energy was calculated by fitting the measured data with the WDD single oscillator model. It was found that the dispersion parameter values  $E_o$  and  $E_d$  of the MEA sample are greater than those in the OEA sample.

## Acknowledgements

This work is partially supported by the Polymer Research Centre at the University of Basrah, for providing us with the necessary examinations and laboratory support.

## References

- [1] Liu X., Cole J. M., Waddell P. G., Lin T. C., Radia J. and Zeidler A., *Molecular origins of optoelectronic properties in coumarin dyes: toward designer solar cell and laser applications*. The Journal of Physical Chemistry A, 116 (2012) 727–737.
- [2] Askim J. R., Mahmoudi M. and Suslick K. S., *Optical sensor arrays for chemical sensing: the optoelectronic nose*. Chemical Society Reviews 42 (2013) 8649–8682.
- [3] Hao S., Wu J., Huang Y. and Lin J., *Natural dyes as photosensitizers for dye-sensitized solar cell*. Solar energy 80 (2006) 209–214.
- [4] Narayan M. R., *Dye sensitized solar cells based on natural photosensitizers*. Renewable and Sustainable Energy Reviews 16 (2012) 208–215.
- [5] Kasiri M. B. and Safapour S., *Natural dyes and antimicrobials for green treatment of textiles*. Environmental chemistry letters 12 (2014) 1–13.
- [6] Crini G., *Non-conventional low-cost adsorbents for dye removal: a review*. Bioresource technology 97 (2006) 1061–1085.
- [7] ZHANG X. and Laursen R. A., *Development of mild extraction methods for the analysis of natural dyes in textiles of historical interest using lc-diode array detector-ms*. Analytical Chemistry 77 (2005) 2022–2025.
- [8] Kant R., *Textile dyeing industry an environmental hazard*. Natural science 4 (2012) 26–30.
- [9] Qin C. and Clark A. E., *DFT characterization of the optical and redox properties of natural pigments relevant to dye-sensitized solar cells*. Chemical physics letters 438 (2007) 26–30.
- [10] Lundqvist M. J., Galoppini E., Meyer G. J. and Persson P., *Calculated optoelectronic properties of ruthenium tris-bipyridine dyes containing oligophenyleneethynylene rigid rod linkers in different chemical environments*. The Journal of Physical Chemistry A 111 (2007) 1487–1497.
- [11] Yoon M. J., *Surface Modifications and Optoelectronic Characterization of TiO<sub>2</sub>-Nanoparticles: Design of New Photo-Electronic Materials*. Journal of the Chinese Chemical Society 56 (2009) 449–454.
- [12] Adeel S., Gulzar T., Azeem M., Saeed M., Hanif I., Iqbal N. et al., *Appraisal of marigold flower based lutein as natural colourant for textile dyeing under the influence of gamma radiations*. Radiation Physics and Chemistry 130 (2017) 35–39.
- [13] Gukowsky J. C., Xie T., Gao S., Qu Y. and He L., *Rapid identification of artificial and natural food colorants with surface enhanced raman spectroscopy*. Food Control 92 (2018) 267–275.
- [14] Lamelas F. and Swaminathan S., *Optical absorption, scattering, and multiple scattering: Experimental measurements using food coloring, india ink, and milk*. American Journal of Physics 88 (2020) 137–140.
- [15] Aburjai T. and Natsheh F. M., *Plants used in cosmetics Phytotherapy Research*. An International Journal Devoted to Pharmacological and Toxicological Evaluation of Natural Product Derivatives 17 (2003) 987–1000.
- [16] Colic M. and Morse D., *The elusive mechanism of the magnetic ‘memory’ of water*. Colloids and Surfaces A: Physicochemical and Engineering Aspects 154 (1999) 167–174.
- [17] Nakagawa J., Hirota N., Kitazawa K. and Shoda M., *Magnetic field enhancement of water vaporization*. Journal of applied physics 86 (1999) 2923–2925.
- [18] Amiri M. C. and Dadkhah A. A., *On reduction in the surface tension of water due to magnetic treatment*. Colloids and Surfaces A: Physicochemical and Engineering Aspects 278 (2006) 252–255.
- [19] Bo D. and XiaoFeng P., *Variations of optic properties of water under action of static magnetic field*. Chinese Science Bulletin 52 3179–3182.
- [20] Holysz L., Szczes A. and Chibowski E., *Effects of a static magnetic field on water and electrolyte solutions*. Journal of Colloid and Interface Science 316 (2007) 996–1002.
- [21] Pang X. F. and Deng B., *The changes of macroscopic features and microscopic structures of water under influence of magnetic field*. Physica B: Condensed Matter 403 (2008) 3571–3577.
- [22] Pang X. and Deng B., *Investigation of changes in properties of water under the action of a magnetic field*. Science in China Series G: Physics, Mechanics and Astronomy 51 (2008) 1621–1632.
- [23] Toledo E. J. L., Ramalho T. C. and Magriotis Z. M., *Influence of magnetic field on physical–chemical properties of the liquid water: Insights from experimental and theoretical models*. Journal of Molecular Structure 888 (2008) 409–415.

- [24] Wang Y., Wei H. and Li Z., *Effect of magnetic field on the physical properties of water*. Results in Physics 8 (2018) 262–267.
- [25] Cefalas A. C., Kobe S., Dražić G., Sarantopoulou E., Kollia Z., Stražišar J. and Meden A., *Nanocrystallization of CaCO<sub>3</sub> at solid/liquid interfaces in magnetic field: A quantum approach*. Applied Surface Science 254 (2008) 6715–6724.
- [26] Del Giudice E., Preparata G. and Vitiello G., *Water as a free electric dipole laser*. Physical review letters 61 (1988) 1085.
- [27] Cefalas A. C., Sarantopoulou E., Kollia Z., Riziotis C., Dražić G., Kobe S., Stražišar J. and Meden A., *Magnetic field trapping in coherent antisymmetric states of liquid water molecular rotors*. Journal of Computational and Theoretical Nanoscience 7 (2010) 1800–1805.
- [28] Higashitani K. and Oshitani J., *Magnetic effects on thickness of adsorbed layer in aqueous solutions evaluated directly by atomic force microscope*. Journal of colloid and interface science 204 (1998) 363–368.
- [29] Kobe S., Dražić G., McGuinness P. J. and Stražišar J., *The influence of the magnetic field on the crystallisation form of calcium carbonate and the testing of a magnetic water-treatment device*. Journal of magnetism and magnetic materials 236 (2001) 71–76.
- [30] Gabrielli C., Jaouhari R., Maurin G. and Keddad M., *Magnetic water treatment for scale prevention*. Water Research 35 (2001) 3249–3259.
- [31] Krems R. V., *Breaking van der Waals molecules with magnetic fields*. Physical review letters 93 (2004) 13201.
- [32] Kumar R., Ali S. A., Mahur A., Virk H., Singh F., Khan S., Avasthi D. and Prasad R., *Study of optical band gap and carbonaceous clusters in swift heavy ion irradiated polymers with uv-vis spectroscopy*. Nuclear Instruments And Methods In Physics Research Section B: Beam Interactions With Materials And Atoms 266 (2008) 1788–1792.
- [33] Srivastava A., Singh V., Aggarwal P., Schneeweiss F., Scherer U. W. and Friedrich W., *Optical studies of insulating polymers for radiation dose monitoring*. Indian J. Pure Appl. Phys. 48 (2010) 782–786.
- [34] Yakuphanoglu F., Cukurovali A. and Yilmaz I., *Determination and analysis of the dispersive optical constants of some organic thin films*. Physica B: Condensed Matter 351 (2004) 53–58.
- [35] Ingle Jr J. D. and Crouch S. R., *Spectrochemical analysis* (Prentice Hall), 1988.
- [36] Dean J. A., *Lange's Hand Book of Chemistry*, McGraw-Hill vol 1583 (McGraw-Hill, Inc.), 1999.
- [37] Yakuphanoglu F., Cukurovali A. and Yilmaz I., *Refractive index and optical absorption properties of the complexes of a cyclobutane containing thiazolyl hydrazone ligand*. Optical Materials 27 (2005) 1363–1368.
- [38] M. Fox, *optical properties of solid*, (Oxford university press), 2010.
- [39] Davidson A., *The effect of the metal atom on the absorption spectra of phthalocyanine films*. The Journal of chemical physics 77 (1982) 168–172.
- [40] Fujii T., Nishikiori H. and Tamura T., *Absorption spectra of rhodamine b dimers in dip-coated thin films prepared by the sol-gel method*. Chemical physics letters 233 (1995) 424–429.
- [41] Tauc J. and Menth A., *States in the gap*. Journal of non-crystalline solids 8 (1972) 569–585.
- [42] Brolo A. G., Gordon R., Leathem B. and Kavanagh K. L., *Surface plasmon sensor based on the enhanced light transmission through arrays of nanoholes in gold films*. Langmuir 20 (2004) 4813–4815.
- [43] Mo L, Yang L and He S, *Acp technical digest*. (OSA), In-proceeding, 2012.
- [44] Neuman K. C. and Block S. M., *Optical trapping*. Review of scientific instruments 75 (2004) 2787–2809.
- [45] Yokogawa S., Burgos S. P. and Atwater H. A., *Plasmonic color filters for cmos image sensor applications*. Nano letters 12 (2012) 4349–4354.
- [46] Shankaran D. R., Gobi K. V. and Miura N., *Recent advancements in surface plasmon resonance immunosensors for detection of small molecules of biomedical, food and environmental interest*. Sensors and Actuators B: Chemical 121 (2007) 158–177.
- [47] Palik E. D., *Handbook of optical constants of solids*, vol 3 (Academic press), 1998
- [48] Wemple S and DiDomenico Jr M, *Behavior of the electronic dielectric constant in covalent and ionic materials*. Physical Review B 3 (1971) 1338.
- [49] Amma D. S. D., Vaidyan V. and Manoj P., *Structural, electrical and optical studies on chemically deposited tin oxide films from inorganic precursors*. Materials chemistry and physics 93 (2005) 194–201.
- [50] Caglar Y., Ilican S. and Caglar M., *Single-oscillator model and determination of optical constants of spray pyrolyzed amorphous SnO<sub>2</sub> thin films*. The European Physical Journal B 58 (2007) 251–256.
- [51] Ilican S., Caglar Y., Caglar M. and Yakuphanoglu F., *Electrical conductivity, optical and structural properties of indium-doped zno nanofiber thin film deposited by spray pyrolysis method*. Physica E: Low-dimensional Systems and Nanostructures 35 (2006) 131–138.